Biochimica et Biophysica Acta, 944 (1988) 399–413
Elsevier

BBA 74161

Conformation and pairing properties of the N-terminal fragments of trichorzianine and alamethicin: a theoretical study

Sylvie Furois-Corbin and Alberte Pullman

Institut de Biologie Physico-Chimique, Laboratoire de Biochimie Théorique associé au C.N.R.S., Paris (France)

(Received 22 April 1988)

Key words: Energy optimization; Alamethicin; Trichorzianine; α-Helix; Glutamine; Proline; (N-terminal fragment)

Energy optimizations are carried out on the N-terminal fragment of trichorzianine in comparison to that of alamethicin. The results indicate that the helical character of the (Ac...Pro^{13}) sequence of trichorzianine (TA IIIc) is essentially alpha with a bend in the helix axis in the end proline region, a structure comparable to the optimal α-helical structure of the corresponding segment (Ac...Pro^{14}) of alamethicin AI. However, two weak $n \rightarrow n+3$ interactions coexist in trichorzianine with the α-helical $n \rightarrow n+4$ hydrogen bonds. The possible role of the glutamine side-chains in pairing such segments together is considered.

Introduction

In a series of recent papers [1–4] we have explored the packing properties of various 'hydrophobic' polypeptide α-helices and their aptitude to form transmembrane bundles with a view to contributing to a better understanding of the capability of such bundles to act as channels or pumps in membranes, a possibility currently considered for explaining the observed properties of physiological transmembrane proteins (e.g. bacteriorhodopsin [5–7], the acetylcholine receptor (for a review see Ref. 8), the sodium channel [9], etc.). Bundles of α-helices have also been considered to play a role in the conductance properties of synthetic polypeptides [10,11] as well as in the case of the natural antibiotic alamethicin [12,13] and of its synthetic analogs [13].

In view of the continuation of our program concerning the formation of channels by helical polypeptides, we consider in this paper a problem encountered in the comparison of alamethicin and trichorzianine.

These molecules are antifungal peptides produced by *Trichoderma viride* and *Trichoderma harzianum fungi* respectively. They both belong to the family of peptaibols, i.e., polypeptides carrying an alcohol at their C-terminal extremity and whose sequence contains a non-classical amino acid, α-aminoisobutyric acid, Aib (an alanine in which the C_α hydrogen atom is substituted by a methyl group). The interest raised by these molecules is due to their antibiotic properties and to their ability to produce membrane modifications [14–18]. Concerning alamethicin, it is well established that it induces voltage-dependent membrane conductance (for a review see Ref. 19). The situation is less clear-cut in the case of trichorzianines. In a recent paper [17] it was shown that the major component of trichorzianines, TA IIIc [20], produces modifications of membrane permeability by inducing leakage of carboxyfluorescein entrapped in vesicles. More recently,

Abbreviations: Ac, acetyl; Aib, α-aminoisobutyric acid; Phcol, phenylalaninol; Trpol, tryptophanol.

Correspondence: A. Pullman, Institut de Biologie Physico-Chimique, Laboratoire de Biochimie Théorique associé au C.N.R.S., 13 rue Pierre et Marie Curie, 75005 Paris, France.

results on macroscopic and single-channel conductance properties of TA IIIc have also been obtained [21], indicating an apparent general pattern of channel formation analogous to that observed with the alamethicins with, however, some differences.

The major components of alamethicin, alamethicin I [22], and of trichorzianine, trichorzianine A IIIc [20], correspond to the sequences (abbreviated here as A and T respectively):

A = AcAib^{1}Pro^{2}Aib^{3}Ala^{4}Aib^{5}Ala^{6}Gln^{7}Aib^{8}Val^{9}Aib^{10}Gly^{11}-Leu^{12}Aib^{13}Pro^{14}Val^{15}Aib^{16}Aib^{17}Glu^{18}Gln^{19}Pheol

T = AcAib^{1}Ala^{2}Ala^{3}Aib^{4}Aib^{5}Gln^{6}Aib^{7}Aib^{8}Aib^{9}Ser^{10}Leu^{11}-Aib^{12}Pro^{13}Val^{14}Aib^{15}Ile^{16}Gln^{17}Gln^{18}Trpol

These two sequences present a number of analogies: high overall hydrophobic character, same number of Aib residues, presence of one glutamine at the first third of the chain and at the end, presence of a proline at the end of the second third of the chain. Perhaps more intriguing are the differences between the two polypeptides, in particular the lack of the proline at the N-terminal in trichorzianine. In order to visualize easily these differences we have aligned the two sequences in Fig. 1, labelling the successive amino-acid positions in alphabetical order starting with 'a' at the N-terminal but labelling 'a'' the second position occupied by a proline in the A sequence and absent in the T sequence. In this fashion, Gln^7 of A coincides in position f with Gln^6 of T, as does Pro^{14} with Pro^{13} in position m, etc. This alignment shows immediately that 12 residues are identical in the two sequences (at positions a, c, d, f, g, i, k, l, m, n, o, r), while Aib b, Ala e, Val h, Gly j, Aib p, Glu q in A are replaced respectively by Ala, Aib, Aib, Ser, Ile, Gln in T. Among the replacements, the most conspicuous are in positions j (where Gly is replaced by a polar residue, Ser) and q (a polar ionic Glu replaced by a polar non-ionic Gln). The replacements in positions h and p substitute a hydrocarbon side-chain for another one, less and more bulky respectively. One notes also that the framed sequence b to e comprises the same four residues in the two molecules with only an interchange in positions b and e. Except for this exchange and for the substitution in position p, the eight Aib residues of both sequences coincide with each other.

As concerns the secondary structure of these molecules, crystal data [12] and NMR studies in solution [23] are available for A. Although differing in their conclusions as to the conformation of the C-terminal part of the molecule, these studies concur in considering that the N-terminal part is α-helical at least up to the 9th or 10th amino acid. Further physico-chemical studies of analogs conclude also to an α-helical structure up to the second proline residue [24].

In the different models [12,24,25] built to explain the voltage-gated conductance of alamethcin a special role is devoted to this N-terminal α-helical segment assumed to insert into the membrane and from aggregates later transformed into bilayer-spanning bundles enclosing a channel. Furthermore, in the model built on the basis of the crystal structure [12], the glutamine side-chains of neighbor α-helices are assumed to favor the packing by forming an array of hydrogen-bonds between their carboxamide groups.

Trichorzianine, much more recently sequenced than alamethicin, has not been the object of many investigations and its conformational studies are less advanced. The only one, to our knowledge, presently available [20] concludes, on the basis of NMR measurements, that this polypeptide is helical up to proline-13 but without definitive information about the overall nature of the helix (α, 3_{10} or other), although it concludes that the first turn of the helix is of the 3_{10} type.

The analogies and differences in the sequence of alamethicin and trichorzianine, as well as the

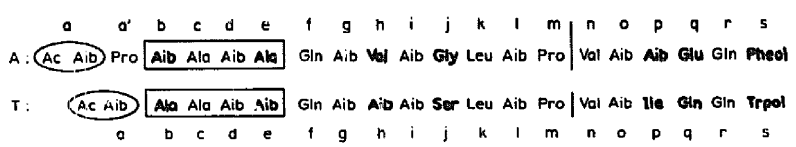

Fig. 1. A diagram emphasizing the analogies and differences in the sequences of alamethicin I (A) and trichorzianine T IIIc (T). The amino acids which differ in the two sequences are in bold type.

apparent differences observed in their conductance, raise the problem of the possible differences in their conformational and aggregation properties. We report in this paper theoretical computations carried out in the same fashion for the two molecules, considering the problem of the nature of the helix in the N-terminal segment of trichorzianine in comparison to that of alamethicin, as well as the possible role of the glutamine and serine side-chains in the pairing of two such segments. We concentrate here on the problems raised by the N-terminal portion of the molecules up to Pro^{14} in alamethicin and to Pro^{13} in trichorzianine since, as mentioned above, this part, according to the models of Refs. 12, 24 and 25, plays a special role in the voltage-dependent conductance.

Standpoint and Methodology

The conformational and aggregation study was conducted using energy optimization computations. The method used (CINFLEX, standing for constrained internal coordinate flexibility) is derived from that employed [26] in our previous studies [1–4], i.e. it relies on the calculation of the energy as a sum of electrostatic, Lennard-Jones, hydrogen-bonding, torsion and polarization components. The electrostatic component is computed using atomic monopoles appropriately optimized so as to reproduce with good accuracy the more accurately computed electrostatic properties of protein constituents [27], and the dispersion and repulsion energies are treated as a Lennard-Jones type interaction with the conventional 6–12 dependance, the case of hydrogen bonds being especially treated so as to account for the angular dependance of these interactions (for the parameters used in the expression of the Lennard-Jones component, see Ref. 26). The CINFLEX methodology, developed in our laboratory [28], allows for the flexibility of rings in an energy optimization procedure, a necessity imposed here by the presence of the proline residue. The angle distorsion force constants used in CINFLEX have been developed by fitting to ab-initio calculations on small model systems (for their values, see Ref. 28). This method allows the backbone dihedral angle ϕ of the proline residue, included in the ring, to be treated as an independent variable.

Considering the N-terminal part of the sequence up to the proline residue, namely T1 = Ac-Aib-Ala-Ala-Aib-Aib-Gln-Aib-Aib-Aib-Ser-Leu-Aib-Pro-$NHCH_3$ (the $NHCH_3$ group was placed after the C-terminal proline in order to mimic the presence of the following amino acid which constrains the rotation about the C_α-C′ bond of this residue), we investigated by energy minimization the preferred helical character of this segment.

The starting conformations for the energy optimization procedures have been chosen as follows:

(a) An entire α-helical conformation with the geometry and dihedral backbone angles of Ref. 29 (ϕ, $\psi = -57.4°$, $-47.5°$), taking into consideration the possible bending effects of the end proline: for the Leu-Aib-Pro C-terminal the initial values of the dihedral angles have been taken from the work of Bosch et al. [30]. The energy of T1 in this starting conformation is more favorable than in a pure α-helix.

(b) In view of the suggestions of Ref. 20:
– an entire 3_{10} helical structure with ϕ, $\psi = -60°$, $-30°$ as currently proposed in the literature for an 'ideal' 3_{10} helix (see, e.g., Refs. 31–33).
– mixed helical conformations: 3_{10} for the first turn and α for the following turns (with the Leu-Aib-Pro C-terminal as in (a)), α for Ac...Gln, followed by 3_{10} for the Aib-Aib-Aib sequence, then α.

For the hydrocarbon side-chains other than those of the Leu-Aib-Pro C-terminal sequence, their $C_\alpha C_\beta$ carbons have been placed in a staggered conformation. Serine was initially placed in a (g^-,t) conformation. In the starting structures, special care has been taken to allow for the many conformational possibilities for the long side-chain of Gln, numerous different initial conformations being used as starting points.

Energy minimizations have been carried out in two different ways, A or B. In procedure A, energy minimization is carried out first by liberating only the side-chains (χ angles) while the backbone is maintained fixed in its starting conformation (ϕ, ψ, ω constant), then the resulting structure is reoptimized with respect to all the dihedral angular variables (all ϕ, ψ, ω and χ) simultaneously. In procedure B, the energy is minimized with respect to all the variables simultaneously, from the start.

For the sake of comparison similar optimizations have been equally carried out in a similar fashion on the N-terminal segment of alamethicin Ac... Pro^{14}, A1 = Ac-Aib-Pro-Aib-Ala-Aib-Ala-Gln-Aib-Val-Aib-Gly-Leu-Aib-Pro-$NHCH_3$, analogous starting points being used in the two cases. (The starting point for the dihedral angles in the early proline-containing segment have been chosen on the basis of preliminary results obtained for the tripeptide CH_3CO-Aib-Pro-$NHCH_3$).

In the first part of the next section we discuss the results of these energy optimizations and their implications. In the second part we consider some of the pairing properties of the optimized segments and the possible role of the glutamine and/or serine residues.

Results and Discussion

I. The helical nature of the trichorzianine N-terminal

The four most stable structures T1a, T1b, T1c and T1d are displayed in Fig. 2. The values of their respective energies and dihedral angles are given in Table I. Both Fig. 2 and the values of the dihedral angles, very similar in the four structures, indicate unequivocally an essentially α-helical character along the whole chain. We shall come back to this point below.

The most conspicuous structural differences between the four structures reside in the conformation of the Gln side-chain which interacts in different ways with the other residues. These differences are indicated by the corresponding values of the χ dihedral angles of Gln in the four structures (Table II).

In T1a and T1d the values of χ_1, χ_2 can be related to the values ($-60°$, $180°$) calculated [34] to provide a good stabilization of the Gln dipeptide and frequently found for Gln residues in the crystallographic structures of globular proteins [35,36]. It corresponds to a partially extended conformation, *'trans'* to the main-chain carbonyl group. The difference between T1a and T1d resides essentially in the difference in the value of χ_3 which allows, in T1d, the formation of a hydrogen bond between the Gln side-chain amide group (residue number 6 in the sequence) and the carbonyl oxygen of residue 2, namely four amino acids below. In view of the energetical difference between T1a and T1d the probability of occurrence of such a conformation of Gln appears non-negligible. This type of hydrogen-bonding between the end group of an nth residue and the $(n-4)$th carbonyl has been noted to occur frequently [37] for the serine, threonine and cysteine residues in α-helical segments of globular proteins and was found as a stable form in our energy

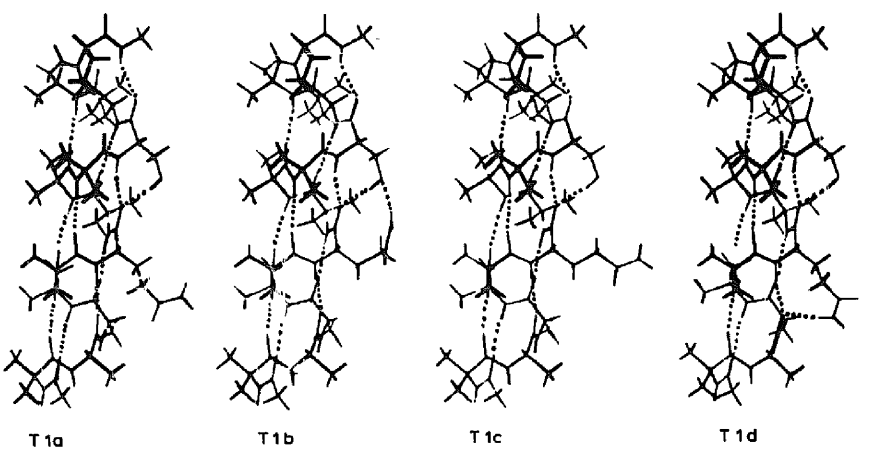

Fig. 2. View perpendicular to the helical axis of the four most stable structures T1a, T1b, T1c and T1d optimized for the (Ac...Pro^{13}), fragment of trichorzianine.

TABLE I

VALUES (IN DEGREES) OF THE DIHEDRAL BACKBONE ANGLES ϕ, ψ, ω IN THE FOUR MOST STABLE CONFORMATIONS T1a, T1b, T1c, T1d

ΔE [a]:	0.0			1.1			2.6			3.6		
Fragment:	T1a			T1b			T1c			T1d		
Residue	ϕ	ψ	ω	ϕ	ψ	ω	ϕ	ψ	ω	ϕ	ψ	ω
Aib[1]	−51.5	−49.9	−177.4	−51.3	−50.2	−175.6	−51.4	−49.9	−175.8	−51.2	−50.3	−174.3
Ala[2]	−56.9	−51.9	174.7	−58.1	−47.6	−176.1	−58.0	−48.4	−175.8	−58.7	−44.7	−177.3
Ala[3]	−56.2	−50.0	−179.5	−59.1	−51.7	−179.8	−59.1	−51.0	−180.3	−61.2	−54.2	−178.6
Aib[4]	−52.8	−54.9	−176.5	−52.9	−54.1	−176.3	−52.6	−54.2	−176.8	−52.6	−53.1	−174.7
Aib[5]	−54.5	−48.4	−175.6	−54.3	−50.4	−175.9	−54.4	−49.4	−175.6	−53.9	−52.2	−174.3
Gln[6]	−58.9	−50.4	−179.0	−57.6	−50.4	−179.1	−58.5	−50.1	−178.8	−60.4	−49.5	−179.3
Aib[7]	−52.3	−56.0	−177.1	−52.0	−56.1	−177.9	−52.2	−56.0	−177.5	−52.0	−55.9	−177.3
Aib[8]	−54.1	−54.0	−172.1	−54.1	−54.2	−171.7	−54.1	−54.0	−172.1	−54.5	−53.9	−172.1
Aib[9]	−56.1	−41.0	−173.8	−56.2	−40.6	−172.8	−56.1	−41.0	−173.7	−55.9	−41.4	−173.8
Ser[10]	−72.9	−53.6	−168.9	−74.7	−52.4	−169.9	−72.9	−53.5	−169.0	−72.8	−53.8	−168.8
Leu[11]	−75.8	−46.2	−167.2	−75.7	−46.1	−167.3	−75.8	−46.2	−167.2	−75.7	−46.0	−167.3
Aib[12]	−59.4	−32.7	−167.9	−59.3	−32.7	−168.0	−59.3	−32.8	−167.8	−59.5	−32.6	−167.7
Pro[13]	−82.7	−43.9	−179.5	−82.7	−43.8	−179.5	−82.7	−43.7	−179.4	−82.7	−44.2	179.6

[a] ΔE is the energy deviation with respect to the most stable structure (energies in kcal/mol, angles in degrees).

optimizations on bundles of hydrophobic helices [4]: the present calculations indicate that it should also be found for Gln. Note that despite the presence of this additional stabilizing hydrogen bond with respect to T1a, T1d remains less stable, the energy loss in the interaction between Gln and some upper residues balancing the gain in stabilizing energy between Gln and the first three residues of the sequence.

In T1b, which follows T1a immediately in term of decreasing stability, the conformation of the Gln side-chain is quite different: here the carboxamide terminal satisfies its hydrogen-binding capability by interacting with the oxygen of the Ser hydroxyl group. Again the hydrogen bond is not sufficient to make T1b more stable than T1a.

Finally, in T1c, the Gln side-chain is com-

TABLE II

CONFORMATIONS OF THE GLUTAMINE AND SERINE SIDE-CHAINS IN T1a, T1b, T1c, T1d

For Gln $\chi_1 = N\text{-}C_\alpha\text{-}C_\beta\text{-}C_\gamma$, $\chi_2 = C_\alpha\text{-}C_\beta\text{-}C_\gamma\text{-}C_\delta$, $\chi_3 = C_\beta\text{-}C_\gamma\text{-}C_\delta\text{-}N_\epsilon$; for Ser $\chi_1 = N\text{-}C_\alpha\text{-}C_\beta\text{-}O_\gamma$, $\chi_2 = C_\alpha\text{-}C_\beta\text{-}O_\gamma\text{-}H(O_\gamma)$, the angles being given in degrees. ΔE as in Table I, in kcal/mol. $A = H(O_\gamma)_{Ser}$, $B = O(C')_{Gln}$, $C = O_{\gamma\ Ser}$, $D = H(N_\epsilon)_{Gln}$, $E = O(C')_{Ala_2}$; $d = H \cdots Q_\gamma$ in Ångströms for the interaction $PH \cdots Q_\gamma$; $\theta = (PH, HQ)$ in degrees.

Structure:	T1a	T1b	T1c	T1d
ΔE:	0.0	1.1	2.6	3.6
Gln χ_1	−73.3	−174.8	−174.8	−77.5
χ_2	170.2	66.2	179.0	171.2
χ_3	75.2	−129.4	−174.1	−74.0
Ser χ_1	−59.4	−55.9	−59.4	−59.6
χ_2	80.3	79.2	79.2	80.7
Hydrogen bonding	A–B d, 2.01; θ, 11.3	A–B d, 1.98; θ, 8 D–C d, 2.2; θ, 19.5	A–B d, 2 θ, 11.5	A–B d, 2.03; θ, 12.3 D–E d, 2.08; θ, 22.8

TABLE III

DIHEDRAL BACKBONE ANGLES (IN DEGREES) IN AN OPTIMIZED SEQUENCE

The sequence used was Ac-Aib[1]-Ala[2]-Aib[3]-Ala[4]-$NHCH_3$. A number of different starting conformations, involving α and 3_{10} helical structures (and for these several sets of dihedral angles), were used. All yielded the same final structure.

Residue	ϕ	ψ	ω
Aib[1]	−51.4	−50.3	−177.1
Ala[2]	−59.8	−48.6	−174.5
Aib[3]	−56.8	−43.2	−179.1
Ala[4]	−67.5	−47.4	178.6

pletely extended in a *'trans'* conformation, *'trans'* to the main-chain nitrogen atom, another of the conformations highly populated in globular proteins [36]. In this conformation the amide group stays away from the polypeptide backbone so that the interactions with the main chain are weakened. The energy difference between T1c and T1d comes essentially from the improved interaction between Ser and Gln in the former.

The side-chain of the serine residue (number 10 in the sequence) existing in T1 (instead of the glycine at the corresponding position in alamethicin) keeps the same conformation in the four structures (Table II): the hydrogen atom of its hydroxyl group is hydrogen-bonded to the backbone carbonyl oxygen of Gln[6], a residue situated four units down in the proceeding turn of the helix. The length and angle of this interaction are quite comparable in the four T1 structures.

Coming back to the details of the dihedral angles ϕ, ψ of the backbone and of the values of ω in the peptide linkages, examination of Table I indicates that:

(a) For a given residue, their values are essentially the same in the four structures, the set of ϕ, ψ, ω varying, however, from one residue to another along the chain. Noteworthy is the fact that this is true even for Gln, which displays considerable variation in its side-chain dihedral angles.

(b) The pair of angles (ϕ, ψ) is not a characteristic of a given amino acid (all Aib's, all Ala's) but it varies according to its location in the chain. The backbone angles of a given short sequence are not necessarily constant either: note that those of Ala[2]Ala[3]Aib[4]Aib[5] in T1 differ from these obtained in the optimal conformation of the same isolated sequence, as shown by the comparison of Tables I and III.

(c) Up to Aib[9], the ϕ, ψ values belong strictly to the α-helical domain. From Ser[10] onwards, larger values of ϕ are observed. The values of ϕ and ψ for Aib[12] are closer to the 'standard' 3_{10} values.

(d) The absolute value of ϕ for Pro[13] is very large: the initial bend adopted in the starting

TABLE IV

CHARACTERISTICS OF THE BACKBONE HYDROGEN BONDS O(C')...H(N) IN T1a, T1b, T1c AND T1d

$d = d$(O...H) in Angströms; θ = (NH, HO) in degrees.

H bond nature	Residues	Fragment							
		T1a		T1b		T1c		T1d	
		d	θ	d	θ	d	θ	d	θ
$n \rightarrow n+3$	Ac ...Ala[3]	2.56	72.1						
$n \rightarrow n+4$	Ac ...Aib[4]	2.00	8.05	2.01	9.30	2.00	8.70	2.02	10.45
$n \rightarrow n+4$	Aib[1] ...Aib[5]	2.05	6.25	2.00	5.18	2.02	5.15	1.97	5.56
$n \rightarrow n+4$	Ala[2] ...Gln[6]	1.92	14.48	1.95	11.77	1.95	14.42	2.11	11.42
$n \rightarrow n+4$	Ala[3] ...Aib[7]	1.96	6.54	1.97	6.52	1.95	6.80	2.01	1.60
$n \rightarrow n+4$	Aib[4] ...Aib[8]	2.08	6.49	2.08	6.92	2.08	6.55	2.01	3.54
$n \rightarrow n+4$	Aib[5] ...Aib[9]	1.96	8.60	1.97	8.62	1.96	8.47	1.98	9.15
$n \rightarrow n+4$	Gln[6] ...Ser[10]	2.08	24.56	2.06	26.19	2.06	24.81	2.07	23.96
$n \rightarrow n+3$	Aib[7] ...Ser[10]	2.55	58.20	2.55	56.66	2.56	58.13	2.58	58.47
$n \rightarrow n+4$	Aib[7] ...Leu[11]	1.96	8.78	1.97	9.40	1.96	9.03	1.96	9.06
$n \rightarrow n+4$	Aib[8] ...Aib[12]	1.96	13.00	1.97	13.03	1.96	12.90	1.96	13.23
$n \rightarrow n+4$	Ser[10]...($NHCH_3$)	2.32	29.88	2.33	29.95	2.34	29.66	2.31	29.79

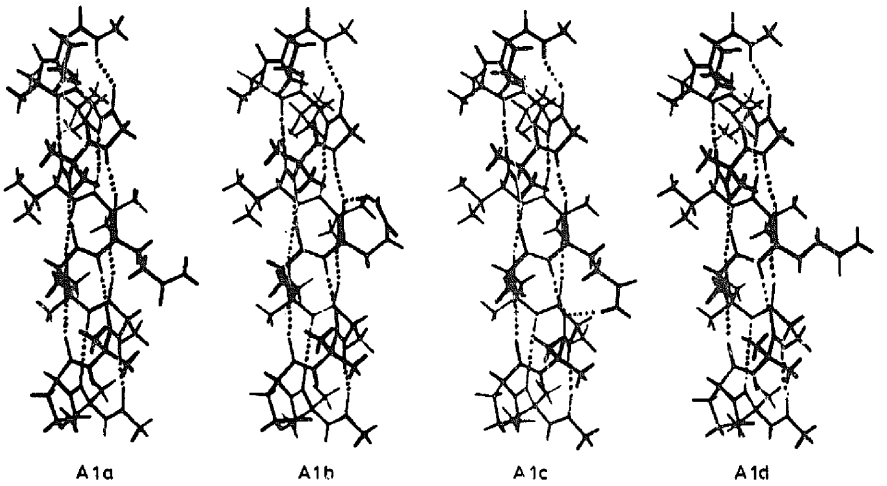

Fig. 3. View perpendicular to the helical axis of the four most stable structures A1a, A1b, A1c and A1d optimized for the (Ac...Pro[14]) fragment of alamethicin.

conformation is enhanced after optimization. Moreover, it is seen that the bend of the structure is in fact already initialized in the Ser[10] region.

(e) The peptide bond is never strictly planar and the departure of ω from 180° is largest for the residues lying in the bent region of the helix.

The characteristics of all the C=O...H-N hydrogen bonds are given in Table IV for the four T1 conformations. This table confirms the α-helical nature of the helix in that all normal α-helical $n \rightarrow n+4$ bonds are present, being similar from one T1 conformation to another, as expected by the similarity of the backbone dihedral angles. Interestingly the $Ala^2 \rightarrow Gln^6$ hydrogen bond is somewhat longer in T1d (which possesses also a hydrogen bond between the Gln side-chain and the carbonyl oxygen of Ala^2) than in the three other T1's. All lengths and angles of these $n \rightarrow n+4$ hydrogen bonds correspond to strong α-helical hydrogen bonds. Note, nevertheless, that interactions occurring in the bent region of the molecule have a greater value of θ, thus are weaker than the other $n \rightarrow n+4$ hydrogen bonds in the molecule.

TABLE V

CONFORMATIONS OF THE GLUTAMINE SIDE-CHAIN IN A1a, A1b, A1c, A1d

χ_1, χ_2, χ_3 of Gln as in Table II. ΔE as in Table I, in kcal/mol; angles in degrees, d in Å.

Structure:	A1a	A1b	A1c	A1d
ΔE:	0.0	0.1	1.6	3.1
$Gln\chi_1$	−73.6	178.7	−77.5	−174.7
χ_2	171.6	62.1	171.7	178.6
χ_3	73.7	−96.1	−76.1	176.3
Hydrogen bonding type	−	+ $O(C')_{Gln}...H(N_\epsilon)_{Gln}$	+ $O(C')_{Aib'}...H(N_\epsilon)_{Gln}$	−
d(O-H)		2.11	2.06	
θ(NH,HO)		35.1	19.9	

TABLE VI

VALUES OF THE DIHEDRAL BACKBONE ANGLES ϕ, ψ, ω IN THE FOUR MOST STABLE CONFORMATIONS A1a, A1b, A1c, A1d

ΔE [a]:	0.0			0.1			1.6			3.1		
Fragment:	A1a			A1b			A1c			A1d		
Residue	ϕ	ψ	ω	ϕ	ψ	ω	ϕ	ψ	ω	ϕ	ψ	ω
Aib[1]	−50.5	−59.0	−167.9	−50.5	−58.5	−169.4	−50.6	−58.0	−170.7	−50.5	−59.1	−169.4
Pro[2]	−58.7	−54.6	−179.1	−57.5	−53.6	−179.1	−56.8	−52.9	−179.1	−56.8	−54.6	−179.1
Aib[3]	−48.8	−57.6	−172.1	−50.3	−53.7	−174.1	−51.7	−50.4	−176.3	−48.9	−57.5	−173.7
Ala[4]	−58.1	−48.7	−179.7	−60.0	−50.4	−178.7	−61.7	−52.9	−176.6	−58.1	−48.7	−179.3
Aib[5]	−52.3	−52.9	−174.7	−52.2	−52.3	−175.0	−52.2	−52.1	−172.9	−52.3	−52.8	−175.4
Ala[6]	−60.8	−45.6	−178.7	−60.1	−47.4	−177.8	−58.5	−49.2	−177.2	−60.8	−45.6	−178.5
Gln[7]	−57.5	−51.1	−177.1	−57.3	−49.5	−177.3	−59.5	−50.5	−177.0	−57.4	−51.2	−176.9
Aib[8]	−53.5	−50.1	−177.3	−54.1	−51.0	−177.1	−52.9	−50.2	−175.5	−53.5	−50.1	−177.4
Val[9]	−61.3	−49.8	−176.1	−61.3	−49.5	−176.5	−62.2	−49.5	−175.9	−61.3	−49.9	−176.1
Aib[10]	−54.4	−42.1	−178.9	−54.2	−41.3	−178.9	−54.2	−42.8	−178.7	−54.5	−42.1	−179.0
Gly[11]	−68.4	−51.5	−170.0	−69.0	−51.6	−170.3	−69.0	−51.6	−170.0	−68.5	−51.5	−170.0
Leu[12]	−67.6	−51.1	−164.1	−67.4	−51.3	−164.1	−67.1	−51.5	−164.1	−67.6	−51.2	−164.1
Aib[13]	−60.5	−33.5	−169.4	−60.3	−33.7	−169.2	−60.5	−33.7	−169.0	−60.4	−33.6	169.3
Pro[14]	−82.2	−43.2	−178.8	−82.3	−40.9	−178.9	−82.2	−41.2	−178.9	−82.2	−41.5	−178.8

[a] As in Table I.

An interesting feature appears upon close scrutinization of Table IV: the existence of a 'hydrogen-bond-like' interaction between the carbonyl oxygen of Aib[7] and the amide hydrogen of Ser[10], thus of an $n \leftarrow n+3$ type, characteristic of a 3_{10} helical structure. However, the length (O...H = 2.55 Å) and angle ($\theta = 58°$) of this interaction are too large to qualify it as a 'real' hydrogen bond. Moreover, the normal α-helical $n \rightarrow n+4$ bond between the same C = O of Aib[7] and H-N of Leu[11] coexists with this supplementary interaction.

Furthermore, a detailed analysis of the first turn of the optimal structure of T1 demonstrates another feature of this kind: the interatomic distance between the carbonyl oxygen of the Ac group and the amide hydrogen of Ala[3] is short compared to all other interactions of this type ($n \rightarrow n+3$): d(O...H) is, in this case, 2.56 Å. Note, however, that this particular interaction in T1 is rather weak as shown by the quite large value (72.1°) of the angle (NH, HO) associated with it (Table IV).

Noteworthy is the fact that all starting conformations used, including entire 3_{10} and $\alpha/3_{10}$ mixed conformations, have yielded the same characteristic α-helical secondary structure of T1. The same is true for the short sequence of Table III.

II. Comparison with the optimal α-helical structure of the corresponding segment (Ac...Pro[14]) of alamethicin A1

We briefly comment below on the essential results obtained for segment A1 of alamethicin. As in the case of T1, the four most stable structures (Fig. 3) found for A1 are very close in energy (Table V) and differ essentially in the conformation of their Gln side-chain. More specifically it appears that:

(a) The helix is essentially α as in the T structures.

(b) The various conformations of the Gln side-chain are closely related to those found in the T1's: same conformation in A1a and T1a, the most stable structures of A1 and T1, respectively; same conformation in A1c and T1d, yielding the same type of hydrogen bond (compare Table V and Table II); overall *'trans'* conformation in A1d and T1c; related conformations in A1b and T1b – in A1b, due to the lack of the serine residue existing in T1, the side-chain of Gln curls back towards the main chain so as to form another type of hydrogen bond, this time between one hydrogen atom of the end amide group and the backbone carbonyl oxygen of the same residue. This conformation corresponds also to a frequently ob-

TABLE VII

CHARACTERISTICS OF HYDROGEN BONDS $O(C')_{residue\ n} \cdots H(N)_{residue\ n+4}$ IN A1a, A1b, A1c AND A1d [a]

Residues	Fragment							
	A1a		A1b		A1c		A1d	
	d	*θ*	*d*	*θ*	*d*	*θ*	*d*	*θ*
Ac...Ala^4	2.04	4.67	2.05	6.68	2.07	9.30	2.05	5.87
Aib^1...Aib^5	1.94	3.29	1.94	3.86	1.93	4.31	1.93	3.65
Pro^2...Ala^6	2.05	10.90	2.00	9.41	1.97	8.55	2.02	10.64
Aib^3...Gln^7	1.94	12.04	1.99	11.42	2.19	9.83	1.97	12.68
Ala^4...Aib^8	1.93	8.31	1.94	9.57	1.98	4.14	1.92	9.27
Aib^5...Val^9	2.14	12.38	2.14	12.13	2.06	10.38	2.15	12.59
Ala^6...Aib^{10}	1.91	10.30	1.91	8.89	1.93	11.61	1.91	9.96
Gln^7...Gly^{11}	2.01	19.97	2.02	22.19	1.99	18.31	2.01	20.13
Aib^8...Leu^{12}	1.94	19.11	1.94	18.57	1.95	19.06	1.94	19.24
Val^9...Aib^{13}	1.91	2.89	1.91	2.64	1.90	1.63	1.91	2.75
Gly^{11}...($NHCH_3$)	2.22	29.58	2.24	29.59	2.22	29.51	2.24	29.68

[a] *d* and *θ* as in Table IV.

served structure in proteins [34]. The various conformations of the Gln side-chains in the optimized A1's and the closeness of their computed energies appear in keeping with the fact that the three alamethicin molecules present in the crystal [12] display different conformations of their Gln side-chains.

(c) The bending effect of the end proline is similar to that of trichorzianine, this bend being already initiated three residues before the proline (see in Table VI the values of the dihedral backbone angles from Gly^{11} onwards). Note that this result correlates remarkably well with that deduced recently from ^{1}H-NMR two-dimensional measurement [38] which suggests a 'tilting' of the helical axis in the region around residues 11–13.

Concerning the effect of proline residues, one can observe, from Table VI, that the Aib^{1}Pro^2 sequence situated at the N-terminal extremity, essentially α-helical, does not adopt the same conformation as the same sequence Aib^{13}Pro^{14} situated at the C-terminal extremity of the segment close to a 3_{10} helical structure. The behavior of proline at the N-terminal agrees with the observation made recently [39] that a great number of α-helical rods in globin molecules have a proline at their N-terminal extremity. In contrast, as seen explicitly in our results, a proline situated within an α-helical structure produces a bend in the helix axis, due to the lack of the amide hydrogen, hence a missing C = O...H-N interaction in the network of the helix hydrogen bonds.

(d) One observes similar strengths of the $n \rightarrow n + 4$ hydrogen bonds (compare Table VII and Table IV), similar from one A1 to another, as expected by the similarity of the backbone dihedral angles.

Apart from these striking similarities an interesting difference exists between T and A in that there exists no 'hydrogen-bond-like' $n \rightarrow n + 3$ in A1 similar to those observed in T1. In particular there is a significant difference between the first turn of A1 and the first turn of T1: *d*(O...H) between Ac and Aib^3 in the former is 3.13 Å, i.e. significantly longer than the corresponding distance (Ac...Ala^3) in T1 (2.56 Å).

In conclusion, the results of this conformational study show that the intrinsically preferred helical character of Ac...Pro^{13} fragment of trichorzianine (TA IIIc) is essentially α with a bend in the helix axis in the end proline region, a conformation fundamentally similar to that of the corresponding sequence of alamethicin. This situation is different from the suggestions of Ref. 20. However, the Ac...Ala^3 interaction in T1 is shorter than the interaction Ac...Aib^3 in A1: it is possible that this interaction, intrinsically weak, might be strengthened under the influence of ex-

ternal factors such as solvents. It remains that the intrinsically preferred helical character of the N-terminal part of T, like that of A, is α.

A final remark concerns the effect of Aib residues on polypeptide conformation. A number of contradictions can be found in the literature concerning this problem (see for instance Refs. 32, 40–44), probably due to the diversity of the sequences considered, of the physical states of the samples, and of the methods of investigation used. Concerning A1, despite its high Aib content, its helical preference is α in a crystalline state [12], in solution [23,38] and in lipid vesicles [45], indicating that the intrinsic preference of the molecule for the α-helix is conserved in the different media. In the case of T1, the intrinsic preference deduced from theoretical computations also appears to be α with a somewhat hidden tendency to become 3_{10} at least partially under appropriate conditions. This is not to say that other sequences could not be intrinsically 3_{10}.

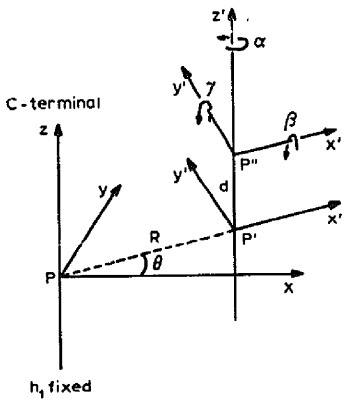

Fig. 4. The six parameters defining the position of a helix h with respect to h_1 in a complex. P is the pivot of h_1 (center of its length). R and θ fix the position of the projection P′ of the pivot P″ on a circle centered at P, α, β and γ define the rotations of h around the directions indicated, d is the vertical translation.

III. The possible role of the polar side-chains in the aggregation of T1 and A1 segments

In the model built to represent the channel made by alamethicin [12], several (Ac...Pro^{14}) N-terminal segments (A1 in the present work) are supposed to pack tightly together with the help of the Gln^7 hydrogen-bonding together parallel α-helices in an aggregate surrounding a central channel. No explicit hypothesis has been made about a possible aggregation of trichorzianines nor about a possible role of its corresponding glutamine residue. The similarities found in Section I both in the conformation of the two segments A1 and T1 and in the conformational behavior of their glutamine residues suggest that similar modes of aggregation could be invoked for the two species. A supplementary interest arises in the case of trichorzianine, due to its possessing another polar group, serine at position 10, capable in principle of hydrogen-bonding to a neighboring helix. Such binding was found in bundles of serine-containing hydrophobic helices [3].

As a preliminary step in the theoretical study of the possible modes of aggregation of these molecules we have considered the pairing properties of the N-terminal segments T1 and A1 and the possible role played in this pairing by their polar residues.

Let us consider the pairing properties of the helical segment T1 considered in Section I, proceeding by energy optimization of a pair of two such helices set initially in one of their most stable conformations. On the basis of the models proposed for alamethicin, we consider here only parallel pairs.

The starting arrangements for the optimization of the pairs have been constructed using the four optimal fragments T1a, T1b, T1c and T1d described in Section I: two identical helices, named h_1 and h_2, were used, h_2 being positioned in space with respect to h_1 by the six parameters defined in Ref. 1 and recalled in Fig. 4. Three values of the interaxial distance R were adopted (9, 10 and 11.5 Å) and, for each R, three rotations of h_2 around its helical axis were performed so as to place its glutamine residue in different orientations with respect to the Gln of h_1 (Fig. 5). The 36 different starting configurations obtained were used as starting points for energy optimization of the pairs proceeding in two steps: (i) In a first step the total energy of the system is minimized with respect to the interhelix variables, maintaining all backbone and side-chain dihedral angles fixed at their opti-

TABLE VIII

ENERGY AND INTERHELIX HYDROGEN-BONDING CHARACTERISTICS OF THE FOUR MOST STABLE T1 PAIRS KEPT STRICTLY PARALLEL

$E_{tot} = E - E_0$ where E is the total optimal energy and E_0 the total energy of the pair when the two helices are at an infinite distance and in their optimal conformation T1a. E_I = total interaction energy including the polarization term. E_I-pol = total interaction energy minus the polarization term. Energies in kcal/mol, d in Angströms. θ in degrees.

Complex	E_{tot}	E_I	E_I-pol	Hydrogen bonds between the two helices		
				atoms involved	d(O...H)	θ(NH,HO)
C1	−6.5	−8.06	−6.87	$H(N_\epsilon)_{(Gln,h_1)}$–$O_{\epsilon(Gln,h_2)}$	2.07	34.0
C2	−6.2	−8.63	−7.73	No interhelix hydrogen-bonding		
C3	−4.84	−9.78	−8.67	$O_{\epsilon(Gln,h_1)}$–$H(N_\epsilon)_{(Gln,h_2)}$	2.14	52.1
C4	−3.95	−11.24	−10.15	$H(N_\epsilon)_{(Gln,h_1)}$–$O_{\epsilon(Gln,h_2)}$	1.96	20.9

mal values found in Section I, except for the χ dihedral angles of Gln and Ser side-chains which were labilized. Constraints were imposed on the interhelical variables so as to maintain the two fragments strictly parallel. (ii) In a second step, the lowest-energy structures resulting from step (i) were reoptimized, labilizing now all intrahelix variables (all dihedral backbone and side-chain angles of h_1 and h_2) and all interhelical variables.

The use of a number of different starting arrangements and of a diversification of the energy-minimization pathway (allowing different trajectories by, for example, various weightings of the translational and rotational parameters, damping of the analytical gradients of the total energy) avoids a number of local energy-minima or artefacts. In this fashion, we can fulfill our purpose, which is not to attain the global minimum (see Refs. 2, 4) but, rather, to obtain arrangements as stable as possible, with a view to examining their properties, particularly the part played by the polar side-chains in their stability.

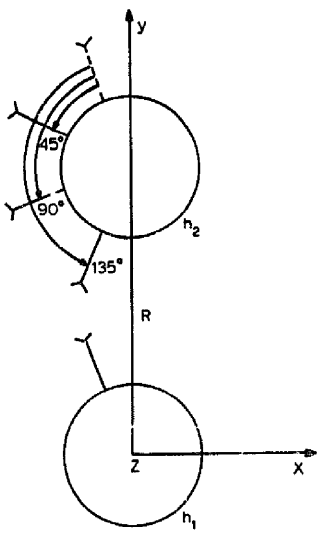

Fig. 5. Schematic representation of the starting arrangements used for the optimization of pairs of T1's. ⊢ represents the Gln side-chain.

Procedure (i) yielded several stable pairs. The energy and interhelix hydrogen-bonding characteristics of the four most stable ones, C1, C2, C3 and C4, are given in Table VIII. It is observed that: – The interaction energy, always negative, is quite favorable in the four pairs, despite the parallel orientation of the two helices. This is true even without the occurrence of a stabilizing hydrogen bond between the two helices (see C2 in Table VIII). As was demonstrated in our previous studies, this is a general feature of the coupling of hydrophobic helices of sufficient length [1,2,4]: the electrostatic component of their interaction energy is positive (as expected by the parallel orientation of the two macro-dipoles) but it is overcompensated by the negative dispersion attraction between the hydrocarbon side-chains of the two partners. (In the case of the couple C1, for instance, inside the total energy, −6.5 kcal/mol given in Table VIII, the electrostatic component is +4.9 kcal/mol while the compensating Lennard-Jones (repulsion/dispersion) term is −11.7. Note that this situation would still be enhanced if a

TABLE IX

ENERGETICAL AND CONFORMATIONAL CHARACTERISTICS OF THE TWO MOST STABLE T1 PAIRS OBTAINED UPON COMPLETE LABILIZATION OF THE SYSTEM

Energies as in Table VIII; distances in Angströms, angles in degrees.

Complex	E_{tot}	E_I	Hydrogen bonds between the two helices			Relative position of the two helices [a]					
			atoms involved	d(O...H)	θ(NH,HO)	R	θ	d	α	β	γ
D1	−15.6	−22.3	$O_{\epsilon(Gln,h_1)}$–$H(N_\epsilon)_{(Gln,h_2)}$	1.95	16.4	9.6	136.4	1.2	40.1	−9.3	−18.5
			$H(N_\epsilon)_{(Gln,h_1)}$–$O_{\gamma(Ser,h_2)}$	2.14	23.0						
D2	−14.5	−17.7	No interhelix hydrogen-bonding			8.4	154.5	−0.8	27.8	−25.6	10.3

[a] See Fig. 4.

dielectric constant was introduced in the calculation, insofar as it acts only by reducing the electrostatic component.)

– Three of the four structures involve hydrogen bonding between the Gln carboxamide groups of the two helices. None involves the Ser side-chains. One has no hydrogen bond at all. In fact a delicate balance occurs between hydrogen bonds and non-bonded interactions: in C3 with an interhelix hydrogen bond weaker (longer d(O...H) and larger θ) than in C1, the interaction energy is more favorable. Also, in C2, with no interhelix hydrogen bond, the interaction energy is more favorable than in C1 and the total energy is nearly as good.

– The absolute value of the total energy E_{tot} is always smaller than that of the interaction energy E_I, implying that the conformational state of h_1 and/or h_2 is always less favorable than when isolated (T1a). Nevertheless this destabilization does not exceed 7.3 kcal/mol in C4. In that case it is shared between the two helices: about 3.6 kcal/mol per helix, practically the energetic destabilization of T1d with respect to T1a (see Table I) due essentially to the difference in conformation of the Gln side-chain. However, the comparison of the energy data in the pairs C1 and C4 shows clearly that the most favorable interaction energy E_I between two helices does not necessarily imply that the pair is the most stable one: to achieve the more favorable value of the interaction energy in C4 each helix has been destabilized to a much greater extent than in C1.

– The polarization component of the interaction is weak (compare E_I and E_I-pol). This was found also in our previous studies on the packing of mainly hydrophobic and uncharged α-helices [1–4].

– In the four structures, the side-chain of the serine keeps the conformation it has in isolated T1 (see Table II).

– The two most stable arrangements (C1, C2) are very close in energy. Nevertheless they correspond to appreciably different packing modes since they differ in the conformation of their Gln side-chains, by the presence or absence of a hydrogen bond

TABLE X

ENERGETICAL AND CONFORMATIONAL CHARACTERISTICS OF TWO A1 PAIRS OPTIMIZED FROM STARTING ARRANGEMENTS MODELLED ON D1 AND D2 RESPECTIVELY

$E_{tot} = E - E_0$ where E is the total optimal energy and E_0 the total energy of the pair when the two helices are at an infinite distance and in their optimal conformation A1a. Other definitions and units as in Tables VIII and IX.

Complex	E_{tot}	E_I	Hydrogen bonds between the two helices			Relative position of the two helices [a]					
			atoms involved	d(O...H)	θ(NH,HO)	R	θ	d	α	β	γ
K1	−20.1	−27.4	$O_{\epsilon(Gln,h_1)}$–$H(N_\epsilon)_{(Gln,h_2)}$	1.97	16.51	8.4	113.6	0 [a]	62.1	26.2	−43.3
K2	−14.5	−16.4	No interhelix hydrogen bonding			8.2	155.4	−2.1	34.3	−41.8	23.3

[a] See Fig. 4.

between the Gln side-chains of the two helices and by the relative orientation of the two helices.

In this first step the helices were maintained strictly parallel. In procedure (ii) this condition is relaxed. In fact, not only the four most stable structures resulting from procedure (i) were reoptimized but also a number of other stable structures obtained from the first step.

Table IX gives the characteristics of the two most stable resulting pairs, D1 and D2. It is seen that the interaction energy between the two fragments has been appreciably increased, due essentially to the labilization of all interhelix variables. In the most stable arrangement, D1, obtained in starting from the C3 conformation, the inclination (see the values of β and γ in Table X) of h_2 with respect to h_1 has allowed an improvement of the hydrogen bond between the two Gln side-chains (see the values of d and θ) and permits, furthermore, the formation of an additional interhelix hydrogen bond between the Gln on h_1 and the Ser oxygen on h_2. However, h_1 is significantly destabilized ($\simeq 5$ kcal/mol) with respect to T1a, essentially owing to the rotation of its Gln side-chain (h_2 is only less favorable than T1a by about 1.8 kcal/mol).

The second most stable pair, D2, results from the reoptimization of C2. As in C2, there is no interhelix hydrogen bond in the final complex, which, however, is very stable: the loss of intrahelix energy is smaller than in D1. In fact, in D2, each helix has practically the conformation and energy of T1b with a destablization of only 0.45 kcal/mol with respect to this structure (and thus less favorable than T1a by only 1.5 kcal/mol), hence a difference of only 1.1 kcal/mol with respect to the most stable pair D1.

It is observed that the Ser side-chains do not make hydrogen bonds between themselves in the most stable pairs. We have obtained an arrangement where such an interaction exists but with a total energy less favorable than in the best pair by 5.7 kcal/mol: to form a hydrogen bond together, the Ser side-chains of both helices must break the stabilizing hydrogen bond initially existing between their hydroxyl hydrogen and the peptide carbonyl oxygen of the Gln residue of the same helix. Furthermore, the hydrogen bond then formed between the two serines is weaker than that achieved, in D1, between the Gln side-chain of h_1 and the Ser side-chain of h_2 (the hydrogen bonding between the two Gln side-chains being similar to that observed in D1).

Having characterized in detail the pairing properties of the N-terminal fragments of trichorzianine we have been able to limit our search of the corresponding fragments of alamethicin to a more rapid study made possible by the results obtained on T1. As a starting point we have placed two optimal A1's in the relative position adopted by the two T1's in D1, then in D2, placing the Gln side-chains in the appropriate conformations. Note, however, that due to he absence of the Ser residue in A1, the Gln side-chains in the starting arrangement modelled on D2 have not the same conformation as those of D2 but the 'corresponding' conformation (see A1b and T1b in section I), i.e. a curling-back of the side-chain of the Gln residue on its own peptide carbonyl oxygen. The energy-minimization computations of these two arrangements yielded two stable pairs K1 and K2, for which the energy and conformational characteristics are given in Table X. As can be seen by comparison of Tables IX and X, the interhelix hydrogen bond occurring between the two Gln side-chains is similar in D1 and K1 but, in this last case, the relative orientation of the two helices has been significantly modified upon optimization (shorter interaxial distance at midheight (R), larger inclination of h_2 with respect to h_1 (β and γ).

In K2 there is, as in D2, no hydrogen bonding between the two Gln side-chains. The interaction-energy component is less favorable by 11 kcal/mol than in K1, whereas for the optimal pairings of two T1's, with and without the Gln hydrogen bonding respectively, this quantity differs by only 4.6 kcal/mol. Due to a better conformational energy, the total energy of K2 is nevertheless less favorable than that of K1 by only 5.6 kcal/mol.

Overall, the pairing properties of the N-terminal fragment (Ac-Pro^{13}) of trichorzianine, and of the corresponding part (Ac...Pro^{14}) of alamethicin, conducted from a comparative point of view, show explicitly the possible role of the polar side-chains of these sequences in their aggregation: in both molecules the most favorable arrangement obtained in the computations is that where the

two Gln side-chain end groups interact by hydrogen bonding. In the most stable pair found for trichorzianine, a hydrogen bond is also formed between the end group of the Ser side-chain of one helix and the end group of the Gln side-chain of the other. However, for this fragment, a stable arrangement without any interhelix hydrogen bond was also found, only 1.1 kcal/mol higher in energy. In the case of alamethicin the corresponding energy difference is larger, favoring the hydrogen-bonded structure by 5.6 kcal/mol.

Concerning the possible role of the Gln side-chains in the aggregation, our results indicate that it can exist, at least in coupling two molecules together, both in trichorzianine and alamethicin. Whether an array of similar bonds can exist between all helices inside a bundle as proposed for alamethicin [12] remains to be demonstrated. We have seen that in our optimal pairs the helices deviate appreciably from the parallelism assumed in the model. It is possible, but yet to be proven, that the presence of other helices in the aggregate and the interaction of each helix with its two neighbors by Gln-hydrogen bonding could impose constraints on the arrangement.

Conclusion

For the reasons explained in the Introduction we have limited the present study to the consideration of the N-terminal part of the molecules in view of the special role it is assumed to play in the voltage-dependent channels of alamethicin.

The optimization of the helical structure of the N-terminal part (Ac...Pro^{13}) of trichorzianine has shown that this helix has an intrinsic preference for an α structure with a small bend initiated about three residues below the proline residue (Pro^{13}). Moreover the comparison of this structure with the optimal corresponding sequence (Ac...Pro^{14}) of alamethicin has stressed the conformational similarity of the two peptides. Nevertheless, in the N-terminal fragment of trichorzianine and coexisting with the standard α-helical $n \rightarrow n+4$ hydrogen bonds, two weak $n \rightarrow n+3$ interactions have been detected. One of them, occurring in the first turn of the sequence, probably explains the conclusion obtained by NMR solution studies that the first turn of trichorzianine is of the 3_{10} type.

We have shown explicitly the appreciable flexibility of the bulky polar Gln side-chain, which can adopt various conformations with little loss in energy. Similar observations were made in our previous studies on Ser side-chains embedded in otherwise hydrophobic sequences [3,4]. This lability, together with the double potentiality for hydrogen bonding of the glutamine residue (which is present in a number of peptaibols akin to alamethicin and trichorzianine and also in some α-helical hydrophobic segments of transmembrane proteins) gives it the ability to play different structural roles in the stability of various bundles and perhaps also in the transfer of ions.

It was shown explicitly that the formation of stable pairs of the α-helical segments considered can occur for trichorzianine and alamethicin in a similar fashion, with a possible (but not indispensable) involvement of the glutamine residues. The present results may lay the foundation for future calculations on bundles of such helices.

References

1 Furois-Corbin, S. and Pullman, A. (1986) Chem. Phys. Lett. 123, 305–310.
2 Furois-Corbin, S. and Pullman, A. (1986) Biochim. Biophys. Acta 860, 165–177.
3 Furois-Corbin, S. and Pullman, A. (1987) J. Biomol. Struct. Dyn. 4, 589–597.
4 Furois-Corbin, S. and Pullman, A. (1987) Biochim. Biophys. Acta 902, 31–45.
5 Henderson, R. and Unwin, P.N.T. (1975) Nature 257, 28–32.
6 Ovchinnikov, Yu.A., Abdulaev, N.G., Feigina, M.Yu., Kiselev, A.V. and Lobanov, N.A. (1979) FEBS Lett. 100, 219–224.
7 Engelman, D.M., Henderson, R., McLachlan, A.D. and Wallace, A.B. (1980) Proc. Natl. Acad. Sci. USA 77, 2023–2027.
8 Popot, J.L. and Changeux, J.P. (1984) Physiol. Rev. 64, 1162–1239.
9 Noda, M., Ikeda, T., Kayano, T., Suauki, H., Takeshima, H., Kurasaki, M., Takahashi, H. and Numa, S. (1986) Nature 320, 188–192.
10 Heitz, F. and Spach, G. (1982) Biochem. Biophys. Res. Commun. 105, 179–185.
11 Heitz, F., Spach, G., Seta, P. and Gavach, C. (1982) Biochem. Biophys. Res. Commun. 107, 481–484.
12 Fox, R.O. and Richards, F.M. (1982) Nature 300, 325–330.
13 Boheim, G., Gelfert, S., Jung, G. and Menestrina, G. (1987)

in Ion Transport through Membranes (Pullman, B. and Yagi, K., eds.), pp. 131–145, Academic Press, Tokyo.
14 Gordon, L.G.M. and Haydon, D.A. (1976) Biochim. Biophys. Acta 436, 541–556.
15 Boheim, G., Janko, K., Leibfritz, D., Ooka, T., Konig, W.A. and Jung, G. (1976) Biochim. Biophys. Acta 433, 182–199.
16 Boheim, G., Irmscher, G. and Jung, G. (1978) Biochim. Biophys. Acta 507, 485–506.
17 Le Doan, T., El Hajji, M., Rebuffat, S., Rajesvari, M.R. and Bodo, M. (1986) Biochim. Biophys. Acta 858, 1–5.
18 Das, M.K., Raghothama, S. and Balaram, P. (1986) Biochemistry 25, 7110–7117.
19 Menestrina, G., Voges, K.P., Jung, G. and Boheim, G. (1986) J. Membrane Biol. 93, 111–132.
20 Bodo, B., Rebuffat S., El Hajji, M. and Davoust, D. (1985) J. Am. Chem. Soc. 107, 6011–6017.
21 Molle, G., Duclohier, M., El Hajji, M., Rebuffat, S., Bodo, B. and Spach, G. (1987) Poster presentation. 9th International Biophysics Congress, Jerusalem, Israel.
22 Pandey, R.C., Cook, J.C. and Rinehart, K.L. (1977) J. Am. Chem. Soc. 99, 8469–8483.
23 Banerjee, U., Tsui, F.P., Balasubramanian, T.N., Marshall, G.R. and Chan, S.I. (1983) J. Mol. Biol. 165, 757–775.
24 Boheim, G., Hanke, W. and Jung, G. (1983) Biophys. Struct. Mech. 9, 181–191.
25 Hall, J.E., Vodyanov, I., Balasubramanian, T.H and Marshall, G.R. (1984) Biophys. J. 45, 233–247.
26 Lavery, R., Sklenar, H., Zakrzewska, K. and Pullman, B. (1986) J. Biomol. Struct. Dyn. 3, 989–1014.
27 Zakrzewska, K. and Pullman, A. (1985) J. Comp. Chem. 6, 265–273.
28 Lavery, R., Parker, I. and Kendrick, J. (1986) J. Biomol. Struct. Dyn. 4, 443–462.
29 Arnott, S. and Dover, S.D. (1967) J. Mol. Biol. 30, 209–212.
30 Bosch, R., Jung, G., Schmitt, H. and Winter, W. (1985) Biopolymers 24, 979–999.
31 Paterson, Y., Rumsey, S.M., Benedetti, G., Nemethy, G. and Scheraga, H.A. (1981) J. Am. Chem. Soc. 103, 2947–2955.
32 Balaram, H., Sukumar, M. and Balaram, P. (1986) Biopolymers 25, 2209–2223.
33 Toniolo, C., Bonora, G.M., Bavoso, A., Benedetti, E., Di Blasio, B., Pavone, V. and Pedone, C. (1986) Biopolymers 22, 205–215.
34 Pullman, B. and Pullman, A. Adv. Protein Chem. 28, 348–526.
35 Janin, J., Wodak, S., Levitt, M. and Maigret, B. (1978) J. Mol. Biol. 125, 357–386.
36 Bhat, T.N., Sasisekharan, V. and Vijayan, M. (1979) Int. J. Pept. Protein Res. 13, 170–184.
37 Gray, T.M. and Matthews, B.W. (1984) J. Mol. Biol. 175, 75–81.
38 Esposito, G., Carver, J.A., Boyd, J. and Campbell, I. (1987) Biochemistry 26, 1043–1050.
39 Schulz, G.E. and Schirmer, R.H. (1979) in Principles of Proteins Structure, 2nd Edn., (Cantor, C.R., ed.), p. 174, Springer Verlag, New York.
40 Burgess, A.W. and Leach, S.J. (1973) Biopolymers 12, 2599–2605.
41 Prasad, B.V. and Sasiesekharan, V. (1979) Macromolecules 12, 1107–1110.
42 Paterson, Y., Stimson, E.R., Evans, D.J., Leach, S.J. and Scheraga, H.A. (1982) Int. J. Pept. Protein Res. 20, 468–480.
43 Bosch, R., Jung, G., Schmitt, H. and Winter, W. (1985) Biopolymers 24, 961–973.
44 Karle, I.L., Sukumar, M. and Balaram, P. (1986) Proc. Natl. Acad. Sci. USA 83, 9284–9288.
45 Jung, G., Bruckner, H. and Schmitt, H. (1981) in Structure and Activity of Natural Peptides (Voelter, W. and Weitzel, G., eds.), pp. 75–114, De Gruyter, Berlin.